© 2017. Published by The Company of Biologists Ltd | Journal of Experimental Biology (2017) 220, 3632-3640 doi:10.1242/jeb.156497

RESEARCH ARTICLE

Long-axis twisting during locomotion of elongate fishes

Cassandra M. Donatelli[1,*], Adam P. Summers[2] and Eric D. Tytell[1]

ABSTRACT

Fish live in a complex world and must actively adapt their swimming behavior to a range of environments. Most studies of swimming kinematics focus on two-dimensional properties related to the bending wave that passes from head to tail. However, fish also twist their bodies three dimensionally around their longitudinal axis as the bending wave passes down the body. We measured and characterized this movement, which we call 'wobble', in six species of elongate fishes (*Anoplarchus insignis*, *Xiphister mucosus*, *Lumpenus sagitta*, *Pholis laeta*, *Apodichthys flavidus* and *Ronquilus jordani*) from three different habitats (intertidal, nearshore and subtidal) using custom video analysis software. Wobble and bending are synchronized, with a phase shift between the wobble wave and bending wave. We found that species from the same habitats swim in similar ways, even if they are more closely related to species from different habitats. In nearshore species, the tail wobbles the most but, in subtidal and intertidal species, the head wobbles more than or the same as the tail. We also wanted to understand the relationship between wobble and the passive mechanics of the fish bodies. Therefore, we measured torsional stiffness and modulus along the body and found that modulus increases from head to tail in all six species. As wobble does not correlate with the passive properties of the body, it may play a different role in swimming behavior of fishes from different habitats.

KEY WORDS: Fish swimming, 3D kinematics, Torsion, Anguilliform

INTRODUCTION

Fish live in a complex and unsteady world. Unlike many animals in a terrestrial environment that maneuver on the surface, an effectively two-dimensional (2D) world, many fishes swim up and down in the water column. Most swimming studies focus only on 2D kinematics. As a result of these studies, properties such as tail beat frequency, stride length and tail beat amplitude have been well characterized (Gillis, 1996; Lauder, 2000, 2015; Liao, 2007; Lauder and Tytell, 2005; Tytell and Lauder, 2004; Tytell et al., 2010; Videler et al., 1999; Webb, 1984). However, very little work has been done on the three-dimensional (3D) movement of fish (Lauder, 2000; Li et al., 2016; Mendelson et al., 2004; Tytell, 2006).

One of the reasons we default to studying swimming in 2D is because it is easy to get repeatable and reliable data that can often be analyzed semi-automatically. 3D data can be difficult and time consuming to gather because of the need to synchronize cameras and track the fish in multiple views. Remarkable progress has been made with semi-automatic tracking and 3D rendering software (Brainerd et al., 2010; Hedrick, 2008; Jackson et al., 2016), yet there is the remaining issue of having the fish swim in an unnatural environment such as a flow tank or small holding area to fit within the view of the calibrated cameras. For our study, we addressed this problem by developing software that tracks the fish using a dorsal camera view and then interpolates 3D kinematics using still images of the fish as a template. This software is almost completely automatic and allows the fish to swim naturally past the camera without any restriction.

In addition, researchers have begun to explore the relationship between mechanical properties and the resulting kinematics (Hebrank et al., 1990; Long et al., 1996; Lucas et al., 2015). For example, Long et al. (1996) found that artificially decreasing the stiffness of the body of a longnose gar significantly decreased its wave speed and tail beat frequency (Long et al., 1996). Others tested flexible plastic foils and found that flapping foils with uniform stiffness propelled themselves more slowly than those with a stiffness gradient from anterior to posterior (Lucas et al., 2015; McHenry et al., 1995). This could mean that a fish might be able to increase their efficiency by tuning their body stiffness along their lengths. Although these studies reveal important information about fish swimming, all of them focus on 2D mechanics and kinematics.

Several studies have noted that fish tend to twist their caudal fin as they move it from side to side (Aleyev, 1977; Lauder, 2000; Tytell, 2006). In particular, Lauder (2000) noted that the dorsal edge leads the ventral edge when the tail beats back and forth, and suggested that the resulting angle of attack could function as a lift-producing mechanism during swimming. Even with this discovery about the potential role of the 3D motion of the tail, biologists and engineers still design underwater devices using simple hinge joints to flap different segments back and forth with no rotation (Barrett et al., 1996; Crespi et al., 2013; Katzschmann et al., 2016; Kopman and Porfiri, 2013; Triantafyllou and Triantafyllou, 1995). The result is devices with performance that pales in comparison to the animals they are inspired by. In elongate fishes, such as eels, gunnels, pricklebacks and others, the body visibly rotates around its long axis during swimming (Fig. 1). This rotation is a torsional wave that we call 'wobble'.

In this study, we therefore examine the kinematics of wobble and its connection to the underlying body mechanics in six species of elongate fishes found in the Salish Sea of the eastern North Pacific. Elongate, eel-like fish body plans have evolved many times among the ray finned fishes (Ward and Brainerd, 2007) and they are found in a wide range of habitats. The fishes we examined occupy three different habitats: the intertidal, which is exposed to the air during low tide; the nearshore, which is from the low tide line to 10 m; and the subtidal, which is from 10 to 300 m (Fig. 2).

We hypothesize that wobble may serve to generate lift in elongate fishes. If wobble is used to generate lift, we would predict that fishes that move up and down more in the water column would wobble more than others. Among the species in this study, the intertidal and subtidal fish spend the majority of their time on the seafloor, with the intertidal species even burrowing under rocks during low tide.

[1]Department of Biology, Tufts University, Medford, MA 02133, USA. [2]Friday Harbor Laboratories, University of Washington, Friday Harbor, WA 98250, USA.

*Author for correspondence (cassandra.donatelli@tufts.edu)

C.M.D., 0000-0001-8641-0681

Received 12 January 2017; Accepted 3 August 2017

Journal of Experimental Biology

Journal of Experimental Biology (2017) 220, 3632-3640 doi:10.1242/jeb.156497

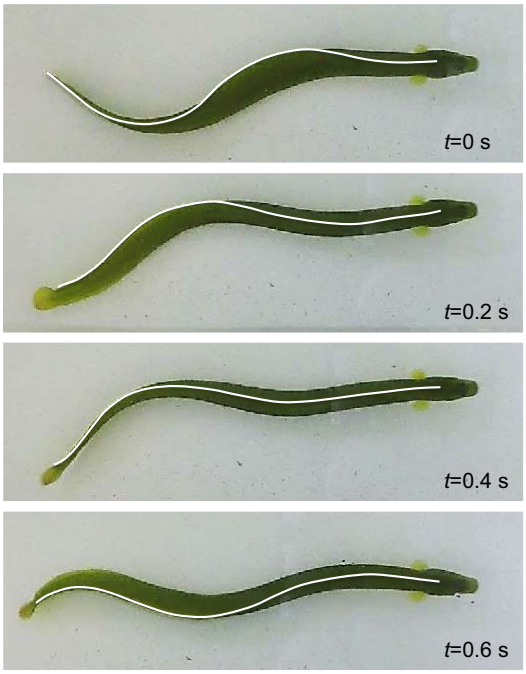

Fig. 1. Time course of *Apodichthys flavidus* swimming over approximately one tail beat. White lines show the trace of the dorsal fin of the animal. Although the fin is the midline of the animal, it does not remain centered above the body of the fish in the frame. This twisting from one extreme to another is wobble.

The nearshore species, however, tend to swim up into the water column more often as they navigate through the eel grass beds where they are most commonly found (Kells et al., 2016; Lamb and Edgell, 2010). If wobble is a motion that produces lift, we would expect the nearshore species to wobble the most to help their negatively buoyant bodies more easily ascend upwards into the water column.

Our study has five specific goals: (1) demonstrate that wobble can be measured in an automated fashion across a range of elongate morphologies; (2) quantify horizontal bending kinematics to test the assumption that body forces are similar across the species; (3) quantify differences in wobble along the length of a fish and among different species; (4) test whether wobble correlates with the torsional stiffness along the length of the body; and (5) correlate wobble with habitat in this group of six elongate fish species.

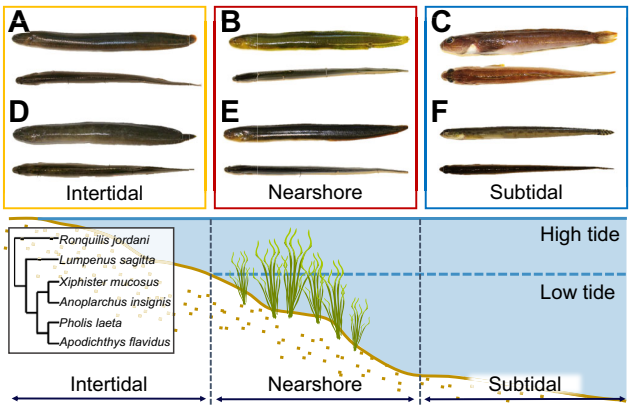

Fig. 2. Fish species and habitat. Top: lateral and dorsal view of the six study species: (A) *Xiphister mucosus*, (B) *Apodichthys flavidus*, (C) *Ronquilus jordani*, (D) *Anoplarchus insignis*, (E) *Pholis laeta* and (F) *Lumpenus sagitta*. The first column (*X. mucosus* and *A. insignis*) are intertidal species, the second column (*A. flavidus* and *P. laeta*) are nearshore species and the last column (*R. jordani* and *L. sagitta*) are subtidal species. Bottom: schematic of habitats. The intertidal zone is the area exposed to air when the tide is out, the nearshore zone is from 0 to 10 m and the subtidal zone is from 10 to 300 m. Inset: phylogeny of the species used (German et al., 2015).

MATERIALS AND METHODS

Experimental procedure

Fish

We gathered data from six species of elongate fishes that were caught in and around the San Juan Islands in WA, USA (Fig. 2). Although all species are considered elongate, they do show some diversity in morphology, especially in fin and head shape. We caught *Anoplarchus insignis* Gilbert and Burke 1912 and *Xiphister mucosus* (Girard 1858) with dip nets and by hand on the beaches surrounding Friday Harbor Laboratories. The majority of *Apodichthys flavidus* Girard 1854, *Pholis laeta* (Cope 1873) and *Lumpenus sagitta* Wilimovsky 1956 were caught in a seine on Jackson Beach in Friday Harbor. *Ronquilus jordani* (Gilbert 1889) were caught with a trawl in the deeper areas surrounding the islands. We housed the fish in the flow-through system at Friday Harbor Laboratories according to the University of Washington's Institutional Animal Care and Use Committee (IACUC) protocol 4238-03.

These particular species, from three families in the Zoarcoidei, live in different habitats (Fig. 2). *Xiphister mucosus* (Stichaeidae) and *A. insignis* (Stichaeidae) are found in the intertidal, often above mean low water under rocks. *Apodichthys flavidus* (Pholidae) and *P. laeta* (Pholidae) are just subtidal, usually captured in algae or seagrass at a depth of a meter or less. They are seldom truly benthic, instead occupying structure off the bottom. *Ronquilus jordani* (Bathymasteridae) and *L. sagitta* (Stichaeidae) are benthic, subtidal fishes found in 10–300 m of water. We collected and measured four to six individuals of each species.

Video data collection

We collected videos of fish in a modified sea table that was part of the same system where the fish were housed. The tank was a track with an oval divider made from acrylic and flexible plastic. The filming area was along the long wall on one side of the track and with a solid white acrylic background. The rest of the tank was off-white. When we moved the fish into the filming tank, they were given 5–10 min to acclimate before the filming started.

For each swimming trial, fish were steered around the track and into the filming area using a movable wall attached to a rod. There was no flow in the track to dictate swimming speed, so fish were allowed to swim freely. They swam around the track until they achieved steady swimming, which was determined post-filming. We characterized a video as steady swimming if the image of the fish moved by about the same distance in each frame and when the trajectory did not change from the beginning to the end of the sequence. During filming, we noted if the fish was not swimming horizontally and discarded those videos. Over 1000 total videos were recorded; of them, only 145 were deemed steady and acceptable for analysis.

We captured videos of steady swimming from above using a GoPro Hero5 Black, with 1080 p resolution and a frame rate of 120 frames s^{-1}. The camera was secured using a mounted tripod above the track and leveled before filming. Because the GoPro lens has a very short focal length, we used the 'narrow' setting on the GoPro during video collection. This digitally decreases the focal length and minimizes distortion. After video collection, the

Journal of Experimental Biology (2017) 220, 3632-3640 doi:10.1242/jeb.156497

remaining fish-eye distortion was corrected using GoPro Studio. Five video sequences for each fish with 3–15 full tail beat cycles per video were analyzed. Following swimming trials, fish were killed with an overdose of MS222. Once killed, we imaged the fish using a Canon Rebel T3 with an 18–55 mm zoom lens.

Torsional stiffness measurements

We measured torsional stiffness using a material testing system (MTS) with a 500N load cell (MTS Synergie 100; MTS Systems, Eden Prairie, MN, USA). After the swimming trials, the same fish were then killed and placed in a custom rig that held the body using 3D printed grippers (Fig. 3). Fish were tested no more than 1 h postmortem to ensure that rigor had not occurred. The first set of grips held the fish body fixed at one point. The MTS load cell pulled a line, which caused the second set of grips to rotate around a bearing. The distance between the two grippers was 10.13 mm for most trials. For estimation of the torsional stiffness, we assumed that the force was at a maximum at the middle of the fish body section between the two grippers. We also assumed that the cross-sectional area of the fish was an ellipse, and that the cross-section was constant between the two grippers. Torsional stiffness (GJ) is defined as:

$$GJ = \frac{Tl}{\alpha}, \tag{1}$$

where T is torque (Nm), l is the distance between the two grippers (m), α is the angle (rad) through which the specimen was twisted, G is the torsional modulus and J is the polar moment of area (m^4), given as:

$$J = \frac{\pi a^3 b^3}{a^2 + b^2}. \tag{2}$$

Here, a is the major radius (height/2; m) and b is the minor radius (width/2; m). We measured this stiffness at several points along the length of the body, taking care not to test any points where the fish may have been damaged by the grippers in a previous trial. We used TestWorks 4.0 (MTS Systems) to control the MTS and specify the angle and speed of rotation.

Video processing

We created software in MATLAB (MathWorks, Natick, MA, USA) to automatically analyze our videos. The code is available on GitHub (https://github.com/CDonatelli/Wobble). It outputs: (1) midlines for each frame of the video; (2) height and width measurements for the fish; (3) processed morphometric, waveform and phase data smoothed using a LOESS (locally weighted scatterplot smoothing) filter; and (4) the 3D kinematic variable we call wobble. Wobble is a dimensionless value that describes the projected width in the camera image, relative to the actual width. It ranges between 0 (fish body completely vertical) and 1 (fish body completely horizontal) and is represented as:

$$W_s = \frac{w_s - d_s}{w_s - h_s}, \tag{3}$$

where W is wobble at each point, s, along the arc of the midline, w is the actual width of the fish at that point, d is the transverse distance, perpendicular to the midline, across the image of the fish in the frame of the camera, and h is the actual fish height. This creates the ratio so that, when d is equal to w (the maximum width of the fish at that point), W is equal to 0 and, when d is equal to h (the maximum height of the fish at that point), W is equal to 1.

To estimate wobble, the software requires measurements of the height and width of the fish at every point along the body. A static dorsal image, taken after swimming trials are completed, is used to measure the width of the fish and a lateral image is used to measure the height at several points along the length of the body. These values are then mapped on to the arc length of the body to estimate wobble. We use a thresholding technique to convert the image to black and white (black background, white fish). The user then specifies where the snout of the fish is on the black and white image, and the software automatically traces the midline of the fish from that point to the tail.

The 2D video processing section of the software uses an intensity threshold to convert each frame to a black and white image. The user identifies the snout on the first frame and then the code automatically tracks the fish for the rest of the frames. For each frame, the software also automatically traces the midline. We accomplished this by first identifying the location of the rest of the fish using the centroid of the thresholded region. The software then examines an arc centered on the previously identified point. It finds the ends of the arc bounded by the white fish and then finds the center of that arc. The center of the new arc is both the next point on the midline and the center point for the next arc. The code records midpoints down the length of the midline until an arc is either entirely in the background or is off the frame. To find the snout in the next frame the code uses the snout point from the previous frame and the centroid parameter again to look in the opposite direction of the centroid for the new snout position.

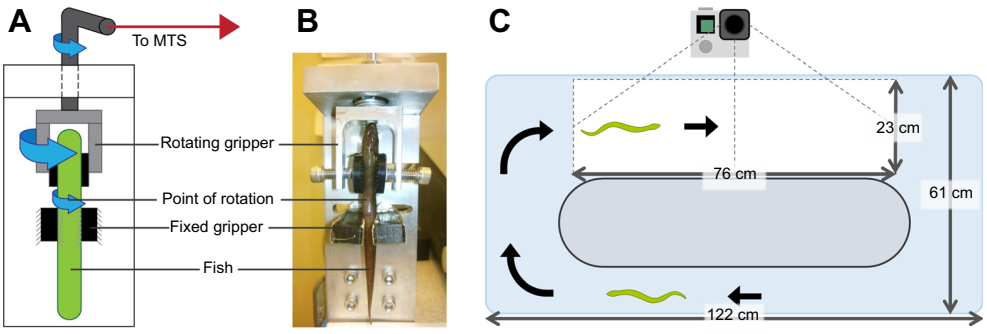

Fig. 3. Schematic of methods. (A) Schematic and (B) photo of the apparatus used to measure torsional stiffness. The fish is held in place by two sets of grippers, one stationary (bottom) and one rotating (top). The angle of rotation is controlled and the force is measured by the material testing system (MTS; not pictured). (C) Schematic of the filming setup. The filming area (white rectangle) was designated by a white piece of acrylic at the bottom of the tank. The fish swam around the track wall (gray oval) and through the filming area. The camera was mounted horizontally above the center of the filming area to minimize distortion.

Journal of Experimental Biology (2017) 220, 3632-3640 doi:10.1242/jeb.156497

Once the midlines are traced for each frame of the video, we move on to the 3D processing. For this step, the software maps the previously identified midlines onto the frames of the color video. The user identifies the color levels (in RGB) of both the fish and the background. The software then proceeds down the length of the fish and plots a line perpendicular to the midline at each point identified along the midline. Using the minimum and maximum color intensities of the fish in the same way as the midline tracer used the arcs, the code identifies the d value for each of those perpendicular lines.

Once all the d values are measured for each frame, we calculate wobble using Eqn 1. The code finishes by smoothing the data using a LOESS filter (MATLAB's smooth function). For our analysis, we chose to measure wobble for five evenly spaced points between the middle of the fish and the tip of the tail, as well as the points where the torsional stiffness was later measured. To generate 3D data using one 2D video, we combined both the measurements taken for each frame of the video with the measurements taken of the still images of the euthanized fish.

We used the results of the code to estimate several 2D kinematic parameters in addition to wobble. Tail amplitude was defined as the distance the tip of the tail traveled [in body lengths (BL)] from one left or right side extreme of the beat to the midpoint of the cycle. Tail beat frequency is the number of tail beat cycles per second (Hz). Wavelength is the distance between the two successive peaks (BL) and wavespeed is the time between these peaks (BL s^{-1}). We defined slip (or slip ratio) as the ratio between swimming speed and wavespeed (Li et al., 2016; Videler, 1993).

Finally, we calculated the phase shift between the bending wave and the wobble wave along the length of the body. Phase shift (ϕ) was calculated as:

$$\phi = \frac{t_{\text{bending}} - t_{\text{wobble}}}{T}, \quad (4)$$

where t_{bending} is the time of the bending peak, t_{wobble} is the time of the wobble peak and T is the period of the bending wave. A phase shift greater than zero will indicate that the bending wave lags behind the wobble wave and a phase shift less than zero will indicate that the bending wave leads the wobble wave.

Statistics

Statistics were done in JMP Pro 12 (SAS Institute, Cary, NC, USA) and MATLAB 2016a. In all plots, error bars and shadows are s.d. To determine significance, we used three different ANOVA models. First, we used separate ANOVAs to test whether tail beat frequency, amplitude or slip depended significantly on swimming speed, habitat, the interaction of swimming speed and habitat, and species nested within habitat. When there was a significant interaction between swimming speed and habitat, which indicated that the slope of the response variable differed among habitats, we did pairwise tests between habitats (nearshore versus intertidal, nearshore versus subtidal, and subtidal versus intertidal) to identify which habitats had different slopes relative to swimming speed. Significance of these multiple-comparison habitat tests was controlled using a Bonferroni correction, which resulted in a critical P value of 0.017. Second, we tested whether wobble, torsional stiffness or the phase lag between bending and wobble differed significantly depending on position along the body, habitat, position crossed with habitat, and species nested within habitat. Finally, we tested whether wobble changed significantly depending on torsional stiffness, habitat, torsional stiffness crossed with habitat, and species nested within habitat.

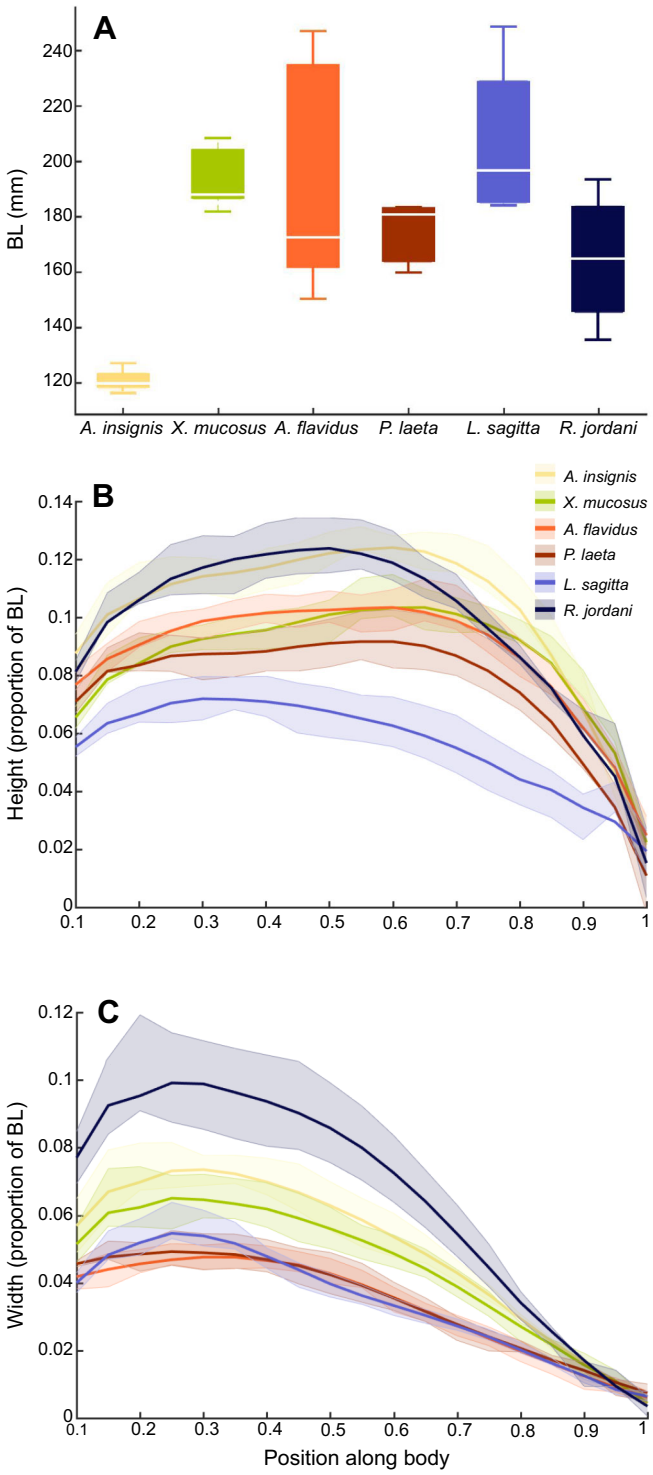

Fig. 4. Morphometrics of the six species of fish in this study. (A) The body lengths (BL) of the individuals used. The center line is the median, and the whiskers represent the 25th and 75th quartiles. (B) Median height profile for all six species. (C) Median width profile of all six species. Along the x-axis, 0 would be the tip of the snout and 1 would be the tip of the tail. Shaded regions indicate s.d.

RESULTS

For all figures, we use a consistent color scheme to indicate the different species. Intertidal species are yellows, nearshore species are reds and subtidal species are blues. For figures with points,

Journal of Experimental Biology (2017) 220, 3632-3640 doi:10.1242/jeb.156497

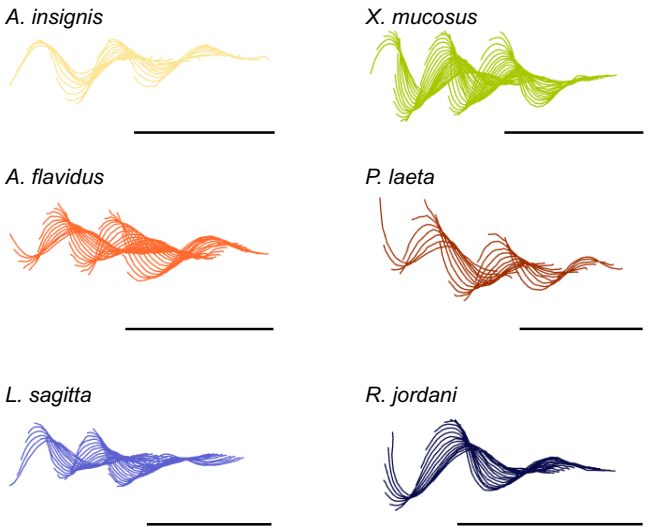

Fig. 5. Midline trace over two tail beats of a representative individual of each species. The black scale bar under each trace is one BL.

intertidal species are circles, nearshore are squares and subtidal are triangles.

Morphometrics

For each of the six species of fish, we measured total body length, as well as an average height and width profile (Fig. 4). The measurements assume the height and width at the tip of the snout are zero. The rest of the measurements are the average across four to six individuals. These results show the different morphologies of the six species. For example, *R. jordani* is wider at the anterior end than the other species and *L. sagitta* is narrower.

2D swimming kinematics

Fig. 5 shows representative digitized midlines for an individual in each of the species, and Fig. 6 shows the summary kinematic parameters. There is a significantly positive relationship between tail beat frequency and swimming speed (P<0.0001) as well as between wave speed and swimming speed (P<0.0001). The overall mean frequency and tail amplitude are different between habitats (P<0.0065 in all cases). Overall, there is no significant relationship between amplitude and swimming speed (P=0.8585), but nearshore and subtidal fishes differ in the slope of the tail beat amplitude relative to swimming speed (P=0.0008). No other slopes are significantly different. The P-values from the ANOVA tests are displayed in Table 1.

Wobble

Fig. 7A shows representative wobble wave traces over two tail beats for *A. flavidus*. Because wobble does not have a sign, there are two wobble wave peaks for each full tail beat cycle, representing wobble to the left and wobble to the right. The wobble wave speed and bending wave speed were equal (Fig. 7B). For the intertidal and nearshore species, wobble tended to increase in amplitude as it traveled down the body (Fig. 7C). The slope of wobble amplitude relative to position was significantly different for all three habitats (P<0.0001). For the subtidal species (*L. sagitta* and *R. jordani*), as well as the nearshore species (*A. insignis*), wobble was much less pronounced. The mean wobble amplitude was significantly different across all habitats (P<0.0001), as well as among species within each habitat (P=0.0024). Table 1 shows the P-values for all tests.

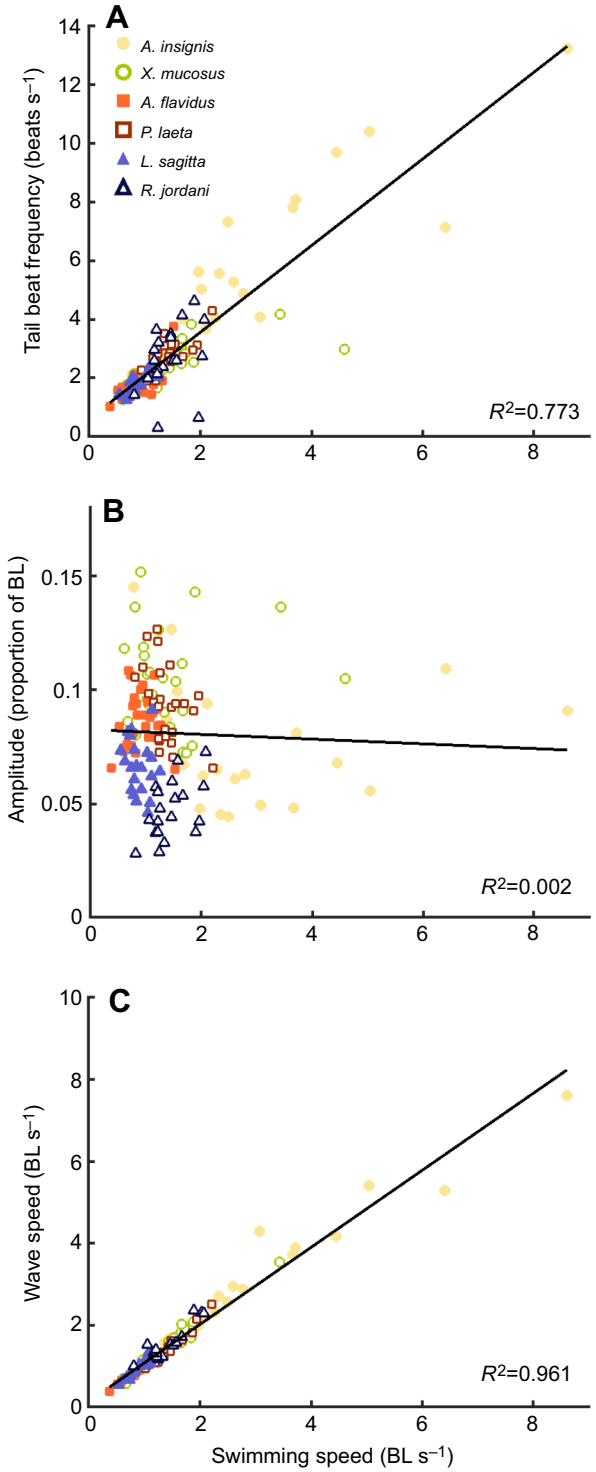

Fig. 6. Relationship between 2D kinematic parameters and swimming speed. (A) Frequency is the number of tail beats per second. (B) Amplitude is the height of the tail beat wave. (C) Wave speed is the speed of the bending wave. Statistics can be found in Table 1.

The phase offset between peak wobble and peak tail beat amplitude varies depending on position along the body and species. There is a single peak in wobble for each half tail beat (Fig. 7A). Fig. 8 shows the phase offset between the wobble peak and the corresponding peak in tail motion. There is a significant effect of habitat on the slope of the line (P=0.0013). The main

Journal of Experimental Biology

Journal of Experimental Biology (2017) 220, 3632-3640 doi:10.1242/jeb.156497

Table 1. Summary statistics

	Effect			
2D kinematics response	Swimming speed	Habitat	Species [habitat]	Habitat×swimming speed
Frequency	**<0.0001**	0.0367	**<0.0001**	0.9583
Wave speed	**<0.0001**	**0.0065**	**0.0036**	0.0204
Amplitude	0.8585	**<0.0001**	**<0.0001**	0.2670
	Effect			
3D kinematics response	Position	Habitat	Species [habitat]	Habitat×position
Wobble	0.3054	**<0.0001**	**0.0024**	**<0.0001**
Torsional modulus	**<0.0001**	0.744	**0.0005**	**0.0013**
Torsional stiffness	0.5893	**<0.0001**	**0.0255**	0.1185
	Modulus	Habitat	Species [habitat]	Habitat×modulus
Wobble	**0.0296**	**<0.0001**	0.0578	**0.0266**
	Stiffness	Habitat	Species [habitat]	Habitat×stiffness
Wobble	0.4075	**0.0029**	0.1022	0.0666

The table shows the *P*-values of 2D kinematics, wobble, torsional stiffness and torsional modulus. Species [habitat] indicates the effect of species nested within habitat. Bold indicates statistical significance.

difference is between nearshore fishes and subtidal fishes (P=0.0005), and there are no significant differences between the other groups.

Torsional stiffness

Fig. 9 shows the relationship between mechanics and kinematics by comparing torsional stiffness and torsional modulus to wobble amplitude along the length of the body. For all species, torsional modulus increases from head to tail (P<0.0001; Fig. 9B) but torsional stiffness does not change significantly (P=0.5893). Mean torsional stiffness (P<0.0029) and modulus (P<0.0001) differ significantly across habitats. Wobble has a much more complex relationship with position along the body (P=0.3054). Effects between groups from different habitats are shown in Fig. 9 and the summary statistics are in Table 1.

DISCUSSION

We gathered both kinematic and mechanical data on six species of elongate fishes native to the Salish Sea in the Pacific Northwest. Although fishes found in the three different habitats swim similarly, there are some notable differences. In particular, amplitudes differ significantly among species and habitats (Fig. 6B). However, all of the species are anguilliform swimmers (Fig. 5), and use the same frequencies and wave speed at the same swimming speed (Fig. 6A,C). Our data are similar in both magnitude and trends to other studies of elongate fishes (D'Aout and Aerts, 1999; Gillis, 1996; Pace and Gibb, 2011; Tytell, 2004), with one notable exception being the tail beat frequency of *A. insignis*, which was higher than studies on eels and other elongate fishes (Fig. 6A). Fishes in different habitats also wobble differently. Overall, subtidal fishes wobble more than intertidal fishes and nearshore fishes tend to wobble more at the tail than at the head (Fig. 7). The relationship between wobble and torsional modulus varies, with a positive relationship in some species and no effect in others (Fig. 9).

Torsional modulus increases towards the tail

As with most elongate fishes, the six species in this study show a decrease in cross-sectional area from head to tail. There has been very little work measuring the torsional properties of biological systems (Arbogast et al., 1997; Vogel, 1992). Some studies on plants (Vogel, 1992) show a range in stiffness measurements similar to ours. We expected that this decrease in cross-sectional area would mean a decrease in the torsional stiffness of the structure if the internal mechanics stayed the same. However, these six species of fish show no change in torsional stiffness from head to tail. The change in distribution of mass (represented by the polar second moment of area J) is similar for all species. The fish have a more circular cross-section at the anterior end, and a more elliptical cross-section at the posterior end. Because J is decreasing along the body, resistance to torsion should also decrease. But torsional stiffness

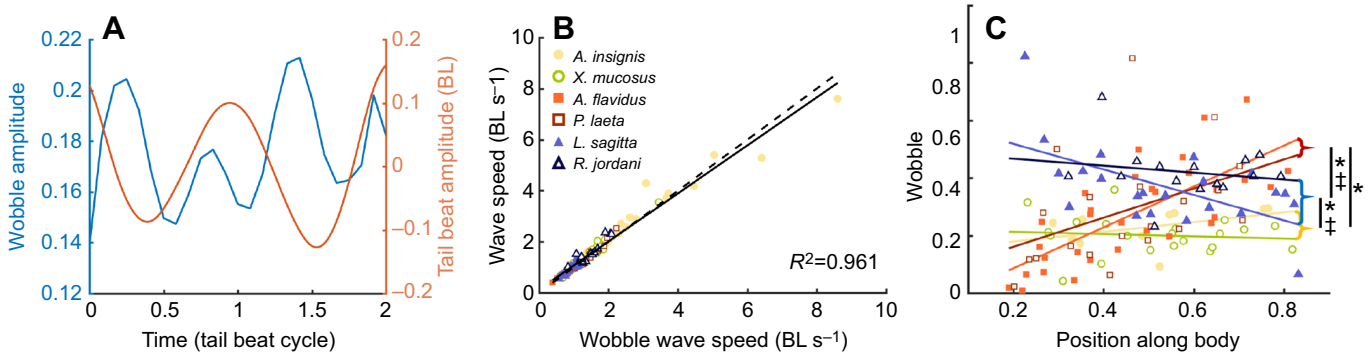

Fig. 7. Characterization of wobble. (A) Representative trace of the wobble wave (blue) and the bending wave (red) over two tail beat cycles. (B) Wobble wave speed versus bending wave speed. The solid line is a regression of the data (R=0.961) and the dashed line is a 1:1 line for comparison. (C) Wobble versus position along the body, where 0 would be the tip of the snout and 1 would be the tip of the tail. Vertical bars indicate statistics between habitats (yellow is intertidal, red is nearshore and blue is subtidal). *Significant difference in slope (P<0.017); ‡difference in mean (P<0.017).

Journal of Experimental Biology

Journal of Experimental Biology (2017) 220, 3632-3640 doi:10.1242/jeb.156497

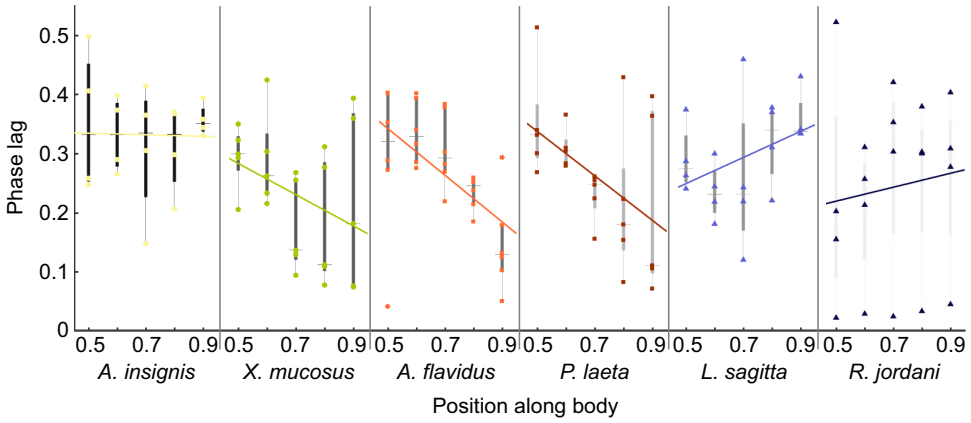

Fig. 8. Phase offsets. Phase offset between the bending wave and the wobble wave along the body. The measurements are taken at five evenly spaced points from 50% down the length of the body (0.5) to the tail (0.9).

remains the same, so the torsional modulus (G) must increase along the length of the body. Having a tail that is more resistant to torsion could give fish some control of the wave as it propagates.

In future work, it will also be important to measure torsional viscoelastic properties. The bodies most likely have damping responses that resist twisting rates. This response would increase the effective torsional modulus proportional to the wobble frequency. If torsional damping differs along the length of the body, this could cause wobble amplitude to vary along the body. Long et al. (2002) and Porter et al. (2016) measured the flexural elastic and damping properties of lamprey bodies and dogfish vertebral columns, respectively, but only on one point along the body. These properties are not known for torsion, nor is it known how they vary along the body.

Wobble cannot be modeled as a mechanical property of the body

Wobble does not have a simple relationship with body mechanical properties. For all species, torsional modulus increases along the body, but wobble amplitude may increase, decrease or stay relatively constant (Fig. 9D). If wobble is a passive result of interactions between the body and the fluid, the lack of correlation between wobble and modulus implies that other aspects of the mechanical interaction differ among the species. Both the kinematics and body shape, although similar among the species, are not identical, and these differences may contribute to differences in wobble. Additionally, differences in mechanical parameters not measured here, such as torsional damping, may produce differences in wobble.

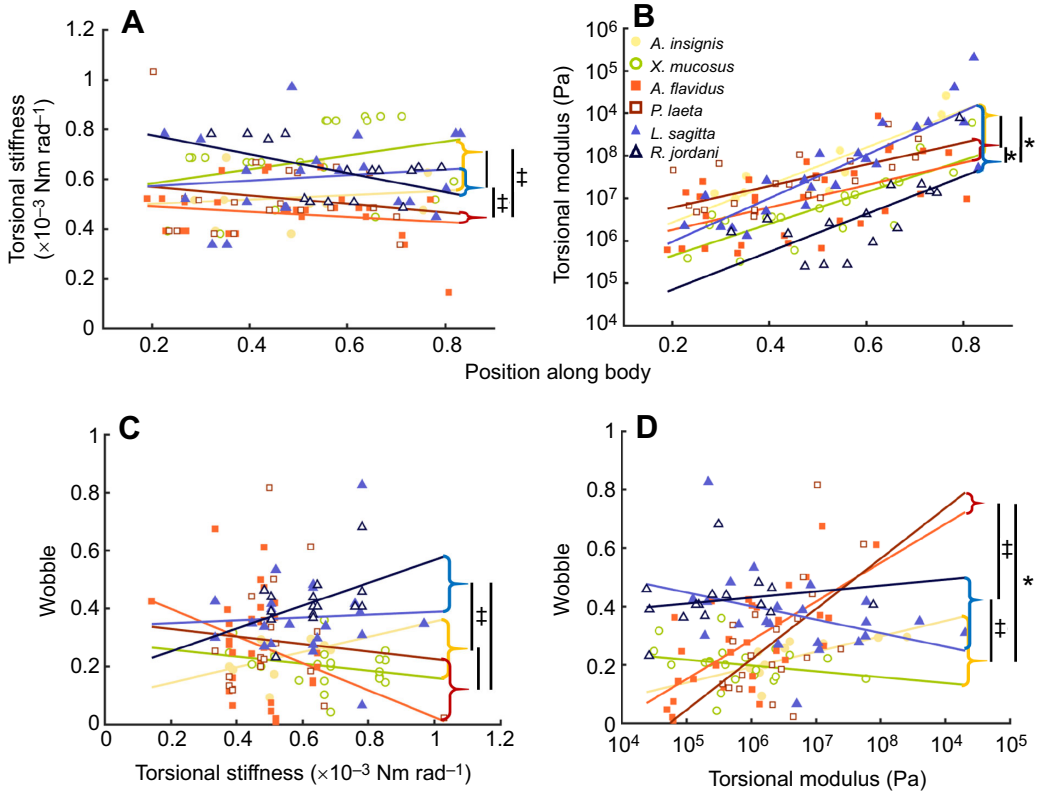

Fig. 9. Mechanical properties. (A) Torsional stiffness (GJ) versus position along the body, where 0 would be the tip of the snout and 1 would be the tip of the tail. (B) Torsional modulus (G) versus position along the body. (C) Wobble versus torsional stiffness. (D) Wobble versus torsional modulus. Vertical bars indicate statistical differences between habitats (yellow is intertidal, red is nearshore and blue is subtidal). *Significant difference in slope (P<0.017); ‡difference in mean (P<0.017).

Wobble could also be actively controlled. Fishes can actively control the erection, side-to-side angle and stiffness of their fins (Chadwell and Ashley-Ross, 2012; Flammang et al., 2013; Lauder and Jayne, 1996). Thus, the elongate fishes in our study could use muscles in their dorsal and anal fins to affect the vortex shedding along the dorsal and ventral margins of the body, which could change the degree of wobble. This hypothesis could be tested by paralyzing the fin ray muscles, which would allow the body to wobble passively. If the degree or pattern of wobble changes, then this test would indicate that the fins are important in the wobble control. Alternatively, fish have been shown to have some independent control over muscle activation in the dorsal and ventral portions of the myotome (Wallén et al., 1985), as well as the ability to produce different amounts of strain in the epaxial and hypaxial regions (Camp and Brainerd, 2014). Slow swimming, like we studied here, is driven by red muscle, which is located in a narrow band along the horizontal midline (Bond, 1996). It may be that fish can control wobble by differentially activating dorsal and ventral portions of the red muscle, but this would require additional testing.

Habitat and wobble are correlated

Regardless of whether wobble is actively or passively controlled, the differences in wobble among species appear to reflect habitat and behavioral differences. Wobble is more correlated among habitats than it is within species in that habitat (Table 1). Among habitats, species differ substantially in both mean and slope (Fig. 7). In particular, nearshore fishes have a wobble wave that increases with amplitude as it passes down the body, whereas the wave amplitude in intertidal fishes stays constant, and the wave in subtidal fishes decreases in amplitude as it is propagated.

We suggest that the large 3D rotations present in the body will lead to the production of lift. Some of the nearshore fish, such as *A. flavidus* and *P. laeta*, have a wobble that approaches 0.6, meaning that, during swimming, parts of their body have an angle of attack greater than 45 deg. Because their cross-section is an ellipse with the major axis in the dorsoventral direction, when wobble approaches 0.6, that part of the body may act like a wing (Dickinson and Götz, 1993). In addition, the phase lag relationship between the wobble wave and the bending wave (Fig. 8) may add to potential lift production. Research on insect wings has shown that a phase lag greater than 1 is associated with a higher lift coefficient (Dickinson et al., 1999). Although much more work is needed on this topic, it is possible that wobble could be involved in lift production in elongate fishes.

Functionally, the lift may be important for maneuvering vertically. The nearshore fishes (*P. laeta* and *A. flavidus*) may wobble in order to use their tails as hydrofoils to produce lift. Their natural behavior involves frequently swimming up off the bottom, rather than mainly skirting along the seafloor like the subtidal fishes, or slithering under rocks like the intertidal fishes. These nearshore fishes are often observed weaving in and out of eel grass beds or coming up to visit night lights (Kells et al., 2016; Lamb and Edgell, 2010). Because of their movement up into the water column, they need to produce more lift, and wobble more than the other fishes. Conversely, the two more benthic species may actively decrease lift at the far ends of their bodies to hold themselves down as they swim across the ocean floor.

Wobble follows different trends for different fish with the same shape

Elongate fish are morphologically conservative, and their locomotion appears similar among species when studied in 2D. Nevertheless, there is functional variation that shows that body form does not determine the swimming style. A close examination of kinematics reveals wobble, an unappreciated contributor to functional diversity in groups that are morphologically similar. It seems certain that a more exhaustive examination of kinematic variables that capture 3D swimming movement will also reveal new correlations with lifestyle, habitat and ecology.

Acknowledgements

We thank Dr Stacy Farina and Dr Stephanie Crofts for their help with the method for measuring wobble during the early stages of the project. In addition, the 2014 Functional Morphology and Ecology of Fishes class at Friday Harbor Laboratories provided advice, feedback and support during the development of the code and recording methods. We also thank the two anonymous reviewers who made substantial contributions to the paper during revisions.

Competing interests

The authors declare no competing or financial interests.

Author contributions

Conceptualization: C.M.D., A.P.S., E.D.T.; Methodology: C.M.D., A.P.S., E.D.T.; Software: C.M.D., A.P.S.; Validation: E.D.T.; Formal analysis: C.M.D., E.D.T.; Investigation: C.M.D.; Resources: A.P.S., E.D.T.; Data curation: C.M.D.; Writing - original draft: C.M.D.; Writing - review & editing: C.M.D., A.P.S., E.D.T.; Visualization: C.M.D.; Funding acquisition: C.M.D., A.P.S.

Funding

This work was supported by a Wainwright fellowship to C.M.D., National Science Foundation grant IOS-1256602 to A.P.S. and National Science Foundation grant RCN-PLS DBI-1062052 to L.J.F. This material is based upon work supported by, or in part by, the US Army Research Laboratory and the US Army Research Office under Contract/Grant No. W911NF-14-1-0268 to E.D.T.

Data availability

The video processing code is available on GitHub (https://github.com/CDonatelli/Wobble). Raw video and numerical data are available upon request.

References

Aleyev, Y. (1977). *Nekton*. The Hague: Junk.

Arbogast, K. B., Thibault, K. L., Scott Pinheiro, B., Winey, K. I. and Margulies, S. S. (1997). A high-frequency shear device for testing soft biological tissues. *J. Biomech.* **30**, 757-759.

Barrett, D., Grosenbaugh, M. and Triantafyllou, M. (1996). The optimal control of a flexible hull robotic undersea vehicle propelled by an oscillating foil. *Proc. Symp. Auton. Underw. Veh. Technol.* 1-9.

Bond, C. E. (1996). *Biology of Fishes*. 2nd revised edition. Pacific Grove: Brooks/Cole.

Brainerd, E. L., Baier, D. B., Gatesy, S. M., Hedrick, T. L., Metzger, K. A., Gilbert, S. L. and Crisco, J. J. (2010). X-ray reconstruction of moving morphology (XROMM): precision, accuracy and applications in comparative biomechanics research. *J. Exp. Zool. A. Ecol. Genet. Physiol.* **313**, 262-279.

Camp, A. L. and Brainerd, E. L. (2014). Role of axial muscles in powering mouth expansion during suction feeding in largemouth bass (Micropterus salmoides). *J. Exp. Biol.* **217**, 1333-1345.

Chadwell, B. A. and Ashley-Ross, M. A. (2012). Musculoskeletal morphology and regionalization within the dorsal and anal fins of bluegill sunfish (Lepomis macrochirus). *J. Morphol.* **273**, 405-422.

Crespi, A., Karakasiliotis, K., Guignard, A. and Ijspeert, A. J. (2013). Salamandra Robotica II: an amphibious robot to study salamander-like swimming and walking gaits. *IEEE Trans. Robot.* **29**, 308-320.

D'Aout, K. and Aerts, P. (1999). A kinematic comparison of forward and backward swimming in the eel anguilla anguilla. *J. Exp. Biol.* **202**, 1511-1521.

Dickinson, M. H. and Götz, K. (1993). Unsteady aerodynamic performance of model wings at low reynolds numbers. *J. exp. Biol.* **174**, 45-64.

Dickinson, M. H., Lehmann, F. O. and Sane, S. P. (1999). Wing rotation and the aerodynamic basis of insect flight. *Science* **284**, 1954-1960.

Flammang, B. E., Alben, S., Madden, P. G. A. and Lauder, G. V. (2013). Functional morphology of the fin rays of teleost fishes. *J. Morphol.* **274**, 1044-1059.

German, D. P., Sung, A., Jhaveri, P. and Agnihotri, R. (2015). More than one way to be an herbivore: convergent evolution of herbivory using different digestive strategies in prickleback fishes (Stichaeidae). *Zoology* **118**, 161-170.

Gillis, G. B. (1996). Undulatory locomotion in elongate aquatic vertebrates: anguilliform swimming since Sir James Gray. *Integr. Comp. Biol.* **36**, 656-665.

Hebrank, J. H., Hebrank, M. R., Long, J. H., Block, B. A. and Wainwright, S. A. (1990). Backbone mechanics of the blue marlin Makaira nigricans (Pisces, Istiophoridae). *J. Exp. Biol.* **148**, 449-459.
Hedrick, T. L. (2008). Software techniques for two- and three-dimensional kinematic measurements of biological and biomimetic systems. *Bioinspir. Biomim.* **3**, 34001.
Jackson, B. E., Evangelista, D. J., Ray, D. D. and Hedrick, T. L. (2016). 3D for the people: multi-camera motion capture in the field with consumer-grade cameras and open source software. *Biol. Open* **5**, 1334-1342.
Katzschmann, R. K., Marchese, A. D. and Rus, D. (2016). Hydraulic autonomous soft robotic fish for 3D swimming. In *Experimental Robotics. Springer Tracts in Advanced Robotics*, Vol. 109 (ed. M. A. Hsieh, O. Khatib, V. Kumar), pp. 405-420. Springer, Cham.
Kells, V., Rocha, L. A. and Allen, L. G. (2016). *A Field Guide to Coastal Fishes from Alaska to California*. Baltimore: Johns Hopkins University Press.
Kopman, V. and Porfiri, M. (2013). Design, modeling, and characterization of a miniature robotic fish for research and education in biomimetics and bioinspiration. *IEEE/ASME Trans. Mechatronics* **18**, 471-483.
Lamb, A. and Edgell, P. (2010). *Coastal Fishes of the Pacific Northwest*, 2nd edn (ed. P. Robson). Maderia Park, BC: Harbour Publishing.
Lauder, G. V. (2000). Function of the caudal fin during locomotion in fishes: kinematics, flow visualization, and evolutionary patterns. *Am. Zool.* **40**, 101-122.
Lauder, G. V. (2015). Fish locomotion: recent advances and new directions. *Ann. Rev. Mar. Sci.* **7**, 521-545.
Lauder, G. V. and Jayne, B. C. (1996). Pectoral fin locomotion in fishes : testing drag-based models using three-dimensional kinematics. *Am. Zool.* **36**, 567-581.
Lauder, G. V. and Tytell, E. D. (2005). Hydrodynamics of undulatory propulsion. In *Fish Biomechanics* (ed. R. E. Shadwick, G. V. Lauder). pp. 425-468. San Diego, CA: Elsevier Academic Press.
Li, G., Müller, U. K., van Leeuwen, J. L. and Liu, H. (2016). Fish larvae exploit edge vortices along their dorsal and ventral fin folds to propel themselves. *J. R. Soc. Interface* **13**, 20160068.
Liao, J. C. (2007). A review of fish swimming mechanics and behaviour in altered flows. *Philos. Trans. R. Soc. London B.* **362**, 1973-1993.
Long, J. H., Hale, M. E., McHenry, M. J. and Westneat, M. W. (1996). Functions of fish skin: Flexural stiffness and steady swimming of longnose gar Lepisosteus osseus. *J. Exp. Biol.* **199**, 2139-2151.
Long, J. H., Koob-Emunds, M., Sinwell, B. and Koob, T. J. (2002). The notochord of hagfish Myxine glutinosa: visco-elastic properties and mechanical functions during steady swimming. *J. Exp. Biol.* **205**, 3819-3831.
Lucas, K. N., Thornycroft, P. J. M., Gemmell, B. J., Colin, S. P., Costello, J. H. and Lauder, G. V. (2015). Effects of non-uniform stiffness on the swimming performance of a passively-flexing, fish-like foil model. *Bioinspir. Biomim.* **10**, 056019.
McHenry, M. J., Pell, C. A. and Long, J. H. (1995). Mechanical control of swimming speed: stiffness and axial wave form in undulating fish models. *J. Exp. Biol.* **198**, 2293-2305.
Mendelson, L., Techet, A. H., Sakakibara, J., Nakagawa, M. and Yoshida, M. (2004). Stereo-PIV study of flow around a maneuvering fish. *Exp. Fluids* **56**, 135.
Pace, C. M. and Gibb, A. C. (2011). Locomotor behavior across an environmental transition in the ropefish, Erpetoichthys calabaricus. *J. Exp. Biol.* **214**, 530-537.
Porter, M. E., Ewoldt, R. H. and Long, J. H. (2016). Automatic control: the vertebral column of dogfish sharks behaves as a continuously variable transmission with smoothly shifting functions. *J. Exp. Biol.* **219**, 2908-2919.
Triantafyllou, M. S. and Triantafyllou, G. S. (1995). An efficient swimming machine. *Sci. Am.* **272**, 64-70.
Tytell, E. D. (2004). The hydrodynamics of eel swimming. II. Effect of swimming speed. *J. Exp. Biol.* **207**, 3265-3279.
Tytell, E. D. (2006). Median fin function in bluegill sunfish, Lepomis macrochirus: Streamwise vortex structure during steady swimming. *J. Exp. Biol.* **209**, 1516-1534.
Tytell, E. D. and Lauder, G. V. (2004). The hydrodynamics of eel swimming. I. Wake structure. *J. Exp. Biol.* **207**, 1825-1841.
Tytell, E. D., Hsu, C.-Y., Williams, T. L., Cohen, A. H. and Fauci, L. J. (2010). Interactions between internal forces, body stiffness, and fluid environment in a neuromechanical model of lamprey swimming. *Proc. Natl. Acad. Sci. USA* **107**, 19832-19837.
Videler, J. J. (1993). *Fish Swimming*. London: Chapman and Hall.
Videler, J. J., Müller, U. K. and Stamhuis, E. J. (1999). Aquatic vertebrate locomotion: wakes from body waves. *J. Exp. Biol.* **202**, 3423-3430.
Vogel, S. (1992). Twist-to-bend ratios and cross-sectional shapes of petioles and stems. *J. Exp. Bot.* **43**, 1527-1532.
Wallén, P., Grillner, S., Feldman, J. L. and Bergelt, S. (1985). Dorsal and ventral myotome motoneurons and their input during fictive locomotion in lamprey. *J. Neurosci.* **5**, 654-661.
Ward, A. B. and Brainerd, E. L. (2007). Evolution of axial patterning in elongate fishes. *Biol. J. Linn. Soc.* **90**, 97-116.
Webb, P. W. (1984). Body form, locomotion and foraging in aquatic vertebrates. *Am. Zool.* **24**, 107-120.